arXiv:1603.06063v1 [cond-mat.soft] 19 Mar 2016

Excluded volume effect in flexible dendron systems: A self-consistent field theory

Meng Shi,[1] Yingzi Yang,[1, a)] and Feng Qiu[1]
State Key Laboratory of Molecular Engineering of Polymers, State Key Laboratory of Computational Physical Science, Department of Macromolecular Science, Fudan University, Shanghai 200433, China

We have studied the conformation and scaling behavior of a flexible dendron (the primary branch of a dendrimer) immersed in neutral or good solvents. A self-consistent field theory combined with a pre-averaged excluded volume potential representing the two-body short-ranged interaction between the monomers, was adopted to calculate the density profile of various generations and branch points thoroughly. Our calculation results support the "dense-core" model. We find the conformation of the dendron is strongly stretched in the densed central region, but much weakly and uniformly stretched in the outer region where the monomer density profile is shoulder shaped. At good solvent limit, both our self-consistent field theory calculation and the Flory mean-field theory calculation give the same scaling law $R \sim (GP)^{1/5}N^{2/5}$, where G is the generation number of the dendron, P is the spacer monomer number, and N is the total monomer number. If we fix G, the scaling law is simplified to $R \sim P^{3/5}$ in good solvent.

Keywords: dendrimer, self-consistent field theory, scaling law

I. INTRODUCTION

Dendrimers are highly branched polymers synthesized generation by generation regularly. Since first prepared in 1978 by Vogtle[1], dendrimer has been extensively studied both experimentally[2–9] and theoretically[10–27] over the past decades for its potential applications in various areas, including sensing, catalysis, molecular electronics[28], biomedicine[28,29] and drug delivery system[30,31], etc. In order to improve the performance of dendrimer in different areas, the physical property is crucial. Especially, the physical property of dendrimers in solutions attracts quite a lot of attentions, because for many applications the dendrimers are immersed in a solvent. However, due to the complex molecular structure and excluded volume effect, the entire conformational property and scaling laws have not yet reached a complete consensus.

(1) **Density profile**: "hollow core" model and "dense-core" model

An early study on the structure of dendrimers was performed by de Gennes and Hervet[10] in 1983. They adopted a self-consistent field theory based on the assumption that "near the center the spacers may behave like flexible coils, but in the outer region they must be elongated"[10]. Thus, the density profile of the dendrimer is minimum at the center and increases towards the edge. This is known as the "hollow-core" model (or "dense-packing" model). This model dominated the understanding on dendrimer for two decades and stimulated a lot application ideas[28], because the model implies a molecular capsule to packing functional drugs for delivery.

However, in 1990, in contrast to the "hollow-core" model, Lescanec and Muthukumar[11] reported a "dense-core" model based on a computer simulation, in which the density profile of the dendrimer is maximum at the center. After that, a great deal of works based on numerical simulation and calculation methods, such as Monte Carlo (MC) simulation[12–14,18–20,23], molecular dynamics (MD)[15,22], Brownian dynamics (BD)[17,21], self-consistent field theory (SCFT)[16,24]and density functional theory (DFT)[32], were published supporting the "dense-core" model. The results of different approaches agree on several features of single dendrimer system. First, the spacers of a small generation number are quite localized, which contributes to a high density peak at the center of dendrimer. Second, with increasing the generation number, a density emerges besides the center density peak, which indicates the dendrimer transfers from a dilute one to a dense one. The experiments of small-angle neutron scattering (SANS), moreover, confirm the "dense-core" model[4,6,33].

Although the "dense-core" model is widely accepted nowadays, a local minimum valley between the center peak and the plateau region in the density profile, first

TABLE I. Summary of scaling laws of dendrimer in solvents

ref	method	scaling law	solvent
11	MC	$R \sim P^{0.5}$ - G fixed	good
		$R \sim N^{0.22}$ - P fixed	good
15	MD	$R \sim N^{0.3}$	good, Θ, poor
18	MC	$R \sim (GP)^{2/5}N^{1/5}$	good
		$R \sim N^{0.3}$	poor
19	MC	$R \sim N^{\frac{1}{3}}$ -small G	good
		$R \sim N^{0.24}$ -large G	good
8	SAXS	$R \sim N^{\frac{1}{3}}$	Methanol
7	SAXS	$R \sim N^{0.42}$ -small G	Methanol
		$R \sim N^{0.21}$ -large G	Methanol

a) Electronic mail: yang_yingzi@fudan.edu.cn

discussed by Mansfield and Klushin[12], remains confusing. This minimum is found in all simulations with strong steric interactions when the generation number G is large enough[2,13,15,19,20], but can disappear when the solvent is good[11,23,34]. The minimum is not found in SCFT calculations where the volume interaction is replaced by a mean-field parameter[16].

(2) **Conformation**: the back-folding phenomenon and the terminal monomer distribution

According to the "hollow-core" model, surface congestion occurs at the periphery of a dendrimer after a certain generation. The spacers are strongly stretched outwards, and consequently the free ends of the last generation distribute near the shell. However, the simulation works supporting "dense-core" model found the terminal monomer spread through the whole dendrimer region[12–15,20,23,34]. This indicates the strong back-folding tendency of the arms of the dendrimer. This phenomenon is confirmed by SANS experiments[6].

(3) **Scaling laws (with solvent)**

The controversy over the scaling laws between the radius of gyration R and other topological parameters of dendrimers, such as the monomer number N, the spacer length P and the generation number G, never stops.

The theoretical approaches predict different power laws in different models. In the "hollow-core" model, De Gennes and Hervet[10] reported $R \sim N^{0.2}$ in good solvent (athermal). In the "dense-core" model, via a mean-field, Flory-type free energy approach[16,18,34], the scaling law is $R \sim N^{1/5}(PG)^{2/5}$ in good solvent and $R \sim N^{1/4}(PG)^{1/4}$ in Θ solvent. In the poor solvent limit, the dendrimer is a dense sphere, so that $R \sim N^{1/3}$.

In computer simulations and experiments, the scaling laws also do not agree with each other, as summarized in Table I. A more detailed table summarizing different power law exponents in theoretical works and simulations can be found in ref.[23].

In order to solve the problems listed above, we perform SCFT to study the conformations and scaling laws of a flexible dendron thoroughly. The SCFT for dendrimer system, first introduced by Boris and Rubinstein[16], adopts a pre-averaged potential to represent the two-body interaction between the monomers. In Flory theory[35], this potential is interpreted as the effect of volume exclusion between the monomers of linear chains in a good solvent. Comparing with MD and MC with full steric interaction, SCFT with the pre-averaged, two-body interaction potential gives good expression of the monomer density profile and the power laws in good solvents, although it is hard to approach the high density limit where three-body interaction plays an important role. Moreover, we study the dendron system instead of a full dendrimer, because the "dendron", defined as the branches at the first level of branching[15,28,36], is the basic building block of dendrimer, and holds all physical properties including the conformation and the power laws of dendrimer. Moreover, in the experiments with an H-shaped core[2,4–6], the dendrimers can be considered as a dendron with the absence of the first generation. The first generation of the dendron mainly contributes to the localized center peak of density[13,15,20] due to its topological position and small volume fraction. Last but not least, dendron is attracting research attentions, such as the segregation of dendrons brushes[22].

Our paper is organized as follows. In Sec. II we introduce the dendron model and the self-consistent field theory with excluded volume potential, and discuss the Flory theory for the dendron. In Sec. III, we focus on the physical aspects (density profile, folding-back conformation, stretching conformation and power laws) of a dendrimer immersed in a good solvent via a detailed analyzing of our simulation data. In the last section, we summarize the main results and draw the conclusion.

II. THEORETICAL METHOD

A. The model

We consider a dendron, the branch at the first level of a dendrimer molecule[15,28,36], immersed in a good solvent. The dendron consists of G generations with the first segment fixed at the origin, as illustrated in Fig.1. We use g to denote the generation number of the spacers. The branch monomer, denoted with a number p, connects the g-th and the $(g+1)$-th spacer. The first monomer and the terminal monomers are denoted as $p = 0$ and $p = G$, respectively. For simplicity, all the spacers, which are assumed to be flexible chains, have the same segment number P. The total segment number is $N = P(2^G - 1)$. We use the square root of the dendron's mean square center-end distance R of a single linear side chain (a no-backward route from $p = 0$ to a terminal monomer $p = G$) of GP monomers to characterize the overall radial size.

In the absence of excluded volume interactions, or in other words, when the dendron is immersed in a Θ solvent, the conformation entropy achieves the maximum value with each linear side chain (a no-backward route from $p = 0$ to one end monomer $p = G$) assuming Gaussian conformation. Therefore, R_0, the square root of the mean square distance from the first monomer $p = 0$ to a terminal monomer $p = G$, is the same as the mean end-to-end distance of a linear Gaussian chain with segment number PG[16,18]

$$R_0 = (PG)^{1/2} a \tag{1}$$

where a is the segment Kuhn length. In Sec. III A, we confirm this power law by SCFT calculation.

B. Flory mean-field theory

We consider the dendron immersed in a good solvent. So that the dendron is not dense. At any spacial point,

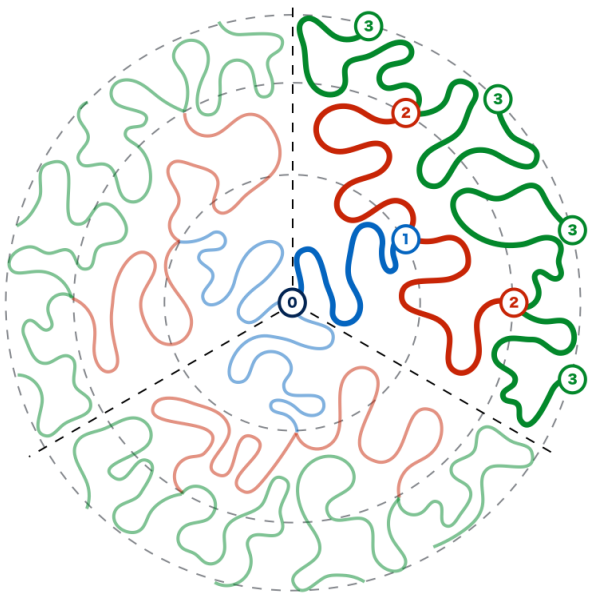

FIG. 1. Illustration of the structure of a G=3 dendrimer. The blue, red, green lines represent the spacers with generation number $g = 1$, $g = 2$, and $g = 3$, respectively. The circles denote the branch monomers and the free end monomers, and the numbers inside the circle are corresponding p values. In our simulation, we only calculate a dendron molecule (the sharp colored area), which is one-third of a dendrimer, in full three-dimensional space.

we assume the local density of the monomer is low. The conformation is determined by the balance between the repulsive excluded volume interaction and the entropic energy. Based on the idea of Flory free energy for a single linear chain in good solvent[35], the free energy of a dendron is,

$$\frac{F}{k_BT} \sim \frac{R^2}{R_0^2} + uN\frac{N}{R^3} \tag{2}$$

where k_B is the Boltzmann constant, T is temperature, u is the mean-field approximated, excluded volume parameter, "$\sim$" means "is proportional to", and the prefactors are neglected.

Comparing Eqn. 2 and the pioneer MF calculations[16,18,34], we modified the calculation in several aspects listed as below.

(1) The free energy Eqn. 2 is based on the whole dendron molecule instead of a linear side chain. Therefore, we assume that the entropic energy of dendron changes proportional to $\frac{R^2}{R_0^2}$. Although not verified by calculation yet, this is still a proper approximation if the stretching conformation does not deviate from the Gaussian chain too much. For the second term on the right side of Eqn. 2, we replace the linear side chain length PG in the pioneer MF calculations[16,18,34] with the total segment number N.

(2) Neglect the three-body interaction term in Sheng *et al.*[18] We assume the monomer density low enough that the three-body interaction is insignificant.

Minimizing the free energy, we obtain a scaling law of the equilibrium size in terms of N, PG and u,

$$R \sim u^{1/5}(PG)^{1/5}N^{2/5} \tag{3}$$

where u is a phenomenological constant to describe the solvent property. We drop u and simplify the power law as $R \sim (PG)^{1/5}N^{2/5}$.

C. Self-consistent field theory

SCFT was first introduced by Edwards and developed by Matsen[37] and Fredrikson[38] et.al. It has been used successfully to study the thermodynamic equilibrium of polymers in its present form. However, the SCFT theory usually does not include the excluded volume interaction, which is absolutely important in dendrimer systems of high generation. Therefore, we modified the theory by including a pre-averaged field $\omega = u\phi$ into the Hamiltonian to approximate the excluded volume interaction, where ϕ is the dimensionless local number density of the segments[39]. The excluded volume of a single segment is characterized[40] by $u\nu_0 = (1-2\chi)\nu_0$, $0 \le \chi \le 0.5$, where χ is the Flory-Huggins parameter between the segment and solvent, and ν_0 is the volume of a segment. So the parameter u describes the overall effect of the volume exclusion of the segments and the swelling of the solvent. At Θ point with $u = 0$, where a slight incompatibility of solvent balances the excluded volume effect of segments, the property of dendron is similar to ideal Gaussian case. As u increases, the size of the dendron expands due to the excluded volume interaction.

The contour parameter of a linear side chain is labeled as s from the initial segment $s = 0$ ($p = 0$) to one free end $s = 1$ ($p = G$). We specify the conformation of the dendron by a vector $\mathbf{r}(s)$ in three-dimensional space. For a given conformation, the Hamiltonian of the system is given by

$$\frac{H}{k_BT} = \frac{3}{2Na^2}\int_0^1 ds\left|\frac{d\mathbf{r}(s)}{ds}\right|^2 + \frac{1}{\nu_0}\int d\mathbf{r}\omega(\mathbf{r})\hat{\phi}(\mathbf{r}) \tag{4}$$

where $\hat{\phi}(\mathbf{r})$ is the dimensionless segment density defined as

$$\hat{\phi}(\mathbf{r}) = N\nu_0\int_0^1 ds\delta(\mathbf{r}-\mathbf{r}(s)) \tag{5}$$

So the partition function could be written as

$$Z \propto \int D\mathbf{r}(s)\exp\left[-\frac{H(\mathbf{r}(s))}{kT}\right] \tag{6}$$

By inserting the the Dirac identity $\int D\Phi\delta(\Phi(\mathbf{r}) - \hat{\phi}(\mathbf{r})) = 1$ and transfer from the particles description to a field description, the partition function is rewritten as

$$Z \propto \int D\Phi\int DW\exp\left\{-\frac{F[\Phi,W]}{kT}\right\} \tag{7}$$

and the free energy functional

$$\frac{F[\Phi,W]}{kT} = -\ln(\frac{Q}{V}) + \frac{1}{\nu_0}\int d\mathbf{r}\omega(\mathbf{r})\Phi(\mathbf{r}) - \frac{1}{N\nu_0}\int d\mathbf{r}W(\mathbf{r})\Phi(\mathbf{r}) \quad (8)$$

$$Q = \int D\mathbf{r}\exp\left\{-\int_0^1 dsW(\mathbf{r}(s)) - \frac{3}{2Na^2}\int_0^1 ds\left|\frac{d\mathbf{r}(s)}{ds}\right|^2\right\} \quad (9)$$

The quantity Q is the partition function of a single Gaussian chain in an (imaginary) external field $W(\mathbf{r})$. Because the functional integral $\int D\Phi\int DW$ is hard to calculate exactly, we therefore adopt the saddle point approximation which takes the most possible configuration as the whole integral. Then, the self-consistent field equations describing the equilibrium behavior of the system are

$$\phi(\mathbf{r}) = \frac{V}{Q}\int dsq(\mathbf{r},s)q^\dagger(\mathbf{r},s) \quad (10)$$

$$\omega(\mathbf{r}) = 2Nu\phi(\mathbf{r}) \quad (11)$$

where $q(\mathbf{r},s)$ is the so-called propagator which represents the probability of finding the s-th segment along the chain at position $\mathbf{r}$ in space. It satisfies the modified diffusion equation

$$\frac{\partial}{\partial s}q(\mathbf{r},s) = \left[\frac{Na^2}{6}\nabla^2 - \omega(\mathbf{r})\right]q(\mathbf{r},s) \quad (12)$$

with the initial condition,

$$q(\mathbf{r},0) = \delta(\mathbf{r}) \quad (13)$$

Calculating a single linear side chain is enough for the dendron system because of its symmetric structure. Therefore the dimensionless density of a dendron could be written as ,

$$\phi(r) = \sum_{g=1}^{G} g\frac{V}{Q}\int_{(g-1)/G}^{g/G} dsq(\mathbf{r},s)q^\dagger(\mathbf{r},s) \quad (14)$$

The numerical calculation process is performed by initiating a complete random field $\omega(\mathbf{r})$, solving the diffusion equation Eqn. 12, calculating the dimensionless density Eqn. 14, generating the new field Eqn. 11, then iterating from the diffusion equation again. Taking the advantage of spherical symmetry of this model, we could reduce the diffusion equation from three dimension into one dimension along the radius r. In spherical coordinate, Eqn. 12 could be rewritten as

$$\frac{\partial}{\partial s}q(r,s) = \frac{Na^2}{6}\frac{1}{r^2}\frac{\partial}{\partial r}r^2\frac{\partial}{\partial r}q(r,s) - \omega(r)q(r,s) \quad (15)$$

In the present work, we adopt the implicit method to solve Eqn. 15 with the boundary condition

$$\left.\frac{\partial q(r,s)}{\partial r}\right|_{r=0} = q(r,s)|_{r=R} = 0 \quad (16)$$

for any $s \neq 0$. During every iteration, the density $\phi(r)$ should be normalized by

$$\int_0^R dr\ 4\pi r^2\phi(r) = N\nu_0 \quad (17)$$

Finally, we could obtain the mean-square end-center distance R^2 from

$$R^2 = \frac{\int dr\ 4\pi r^2 q(r,1)r^2}{\int dr\ 4\pi r^2 q(r,1)} \quad (18)$$

In this paper, we choose the Kuhn length a and the segment volume ν_0 as units.

III. RESULTS AND DISCUSSION

In this section, we exhibit the SCFT calculation results of dendron systems by systematically changing the parameters $2 \leq g \leq 10$, $1 \leq P \leq 20$, and $0 \leq u \leq 0.2$. We first discuss the Gaussian dendron to verify the power law of R_0 as well as to prove the validity of our calculation. Second, we analyze the density profiles of the dendron with different u to show the response of conformation to the solvent property and the excluded volume effect. Third, we discuss the elongated conformation of spacers of different topological positions. At last, we compare the scaling laws obtained from SCFT and Flory mean-field theory.

A. Ideal Gaussian dendron

The ideal Gaussian dendron with $u = 0$ is the simplest case that the segments are "ghost" segments and do not interact via volume exclusion. A linear side chain of length PG behaves as an ideal linear chain, because the conformation of the branches has no influence to it. Therefore, the center-end distance R_0 obeys the power law in Eqn. 1, and the end monomer distribution $\Psi(r)$ can be obtained analytically,

$$\Psi(r) = \left(\frac{3}{2PGa^2}\right)^{\frac{3}{2}}\exp\left\{-\frac{3r^2}{2PGa^2}\right\} \quad (19)$$

As shown in Fig. 2(a), our results reproduce the power law in Eqn. 1 very well within an error less than 1%, which we attribute to the accuracy of spacial discretization in the calculation. And $\Psi(r)$ obtained in the calculation overlaps the theoretical result Eqn. 19 totally in Fig. 2(b). Therefore, we believe that our SCFT approach is appropriate for the dendron system.

B. Density profile of dendron

The segment density of a single dendrimer attracts quite a lot of theoretical as well as experimental research interest, because it reflects the conformation of

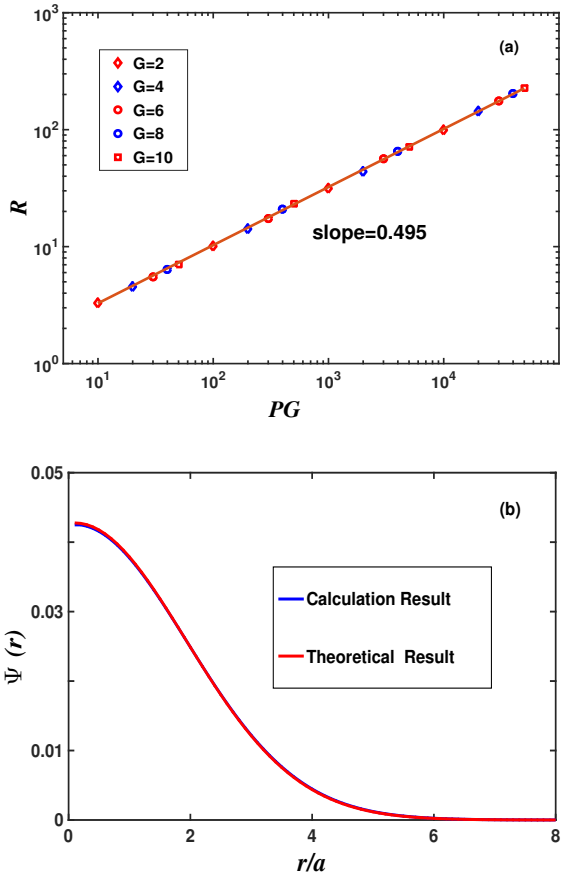

FIG. 2. (a)Scaling laws for ideal Gaussian dendron of $G = 2, 4, 6, 8, 10$ with $P = 5, 50, 500, 5000$. (b)The probability density distribution $\Psi(r)$ for the center-to-end vector of an ideal dendron with $G = 2$ and $P = 5$.

the molecule. We can design the function of a dendrimer if we have accurate knowledge of the spacial position of each monomer.

We analyze the total segment number density of the dendron of generation G, $\rho_G(r)$, which obeys $\int dr\rho_G(r)4\pi r^2 = N$, as shown in Fig. 3 . Obviously, the monotonically decreasing density profile with the highest density at $r = 0$ supports the "dense-core" model[11]. With increasing u, the shape of $\rho_G(r)$ transfers from the fast decreasing mode of $u = 0$, to a typical "dense-core" model density profile with a center peak and a plateau region[13–15,19,20,34].

Comparing with the system in a Θ solvent($u = 0.0$), $\rho_G(r)$ exhibits an obvious penetration of segments into the solvent even though u only slightly increases to 0.001. For $\rho_G(r)$ with $u \geq 0.01$, a "shoulder" of very slow decreasing rate emerges. The region size of the shoulder increases with u, reflects stronger extension of the dendron with increasing excluded volume effect (or in other words, the swelling behavior of the dendron in good solvent). The emergence of the "shoulder" agrees the result of MD and MC simulations with full volume exclusion[13–15,19,20],

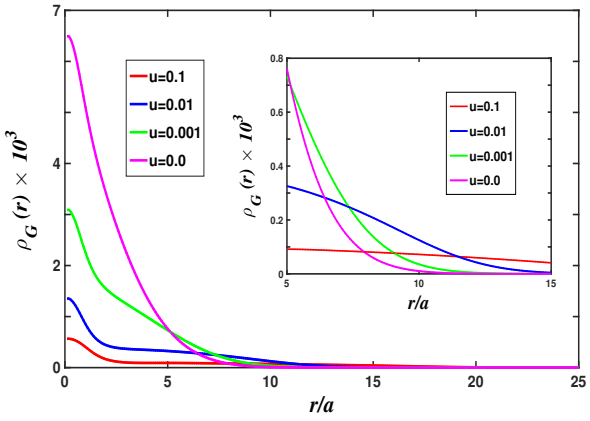

FIG. 3. The total segment number density $\rho_G(r)$ of the dendron with $G = 6$, $P = 5$, and $u = 0.0, 0.001, 0.01, 0.1$. The inset is the magnification of the region of $5 \leq r/a \leq 15$.

as well as the previous MF theory calculations with pre-averaged volume exclusion effect[34].

However, the local minimum value between the center peak and the shoulder region never appears in our SCFT calculation. Note that this phenomenon disappears when the solvent is good[11,23,34]. Moreover, the minimum is also not found in self-consist mean-field theory calculations[16], where the volume interaction energy only keeps two-body interaction term and neglects higher orders. Therefore, we attribute the arising of the local density minimum to the innegligible three-body interactions of volume exclusion, which means the dense dendron beyond our low-density assumption.

In order to clarify the distribution of different generations to the total density profile, we analyze the segment number density $\rho_g(r)$ of g-th generation spacers, which obeys $\int dr\rho_g(r)4\pi r^2 = 2^{g-1}P$. As shown in Fig.4(a), the density peak near the center is mostly contributed by the first generation $g = 1$, while the other generations consist the shoulder after the sharp peak at the center. In Fig.4(a), when the generations $g \geq 4$, the monomers in higher generations comprise the ones in lower generations. This is identical to the result obtained by Murat and Grest[15]. The position of the peak moves outwards with increasing g except the last generation due to the free terminal monomer. Also, any changes of the dendron parameters which will increase the excluded volume energy, *i.e.* the increasing of u (Fig. 4(b)) and the increasing of the generation number G of dendron (Fig. 5), will move the $\rho_g(r)$ to larger r.

Although $\rho_g(r)$ of different g spreads more outwards with increasing generation number, it always has non-vanishing value at the center. Particularly, the outmost generation $g_{g=6}(r)$ distributes over the whole dendron region (Fig.4(b)). The non-vanishing value of $\rho_{g\geq 2}$ indicate a strong back-folding conformation, a phenomenon we will discuss in detail in next section.

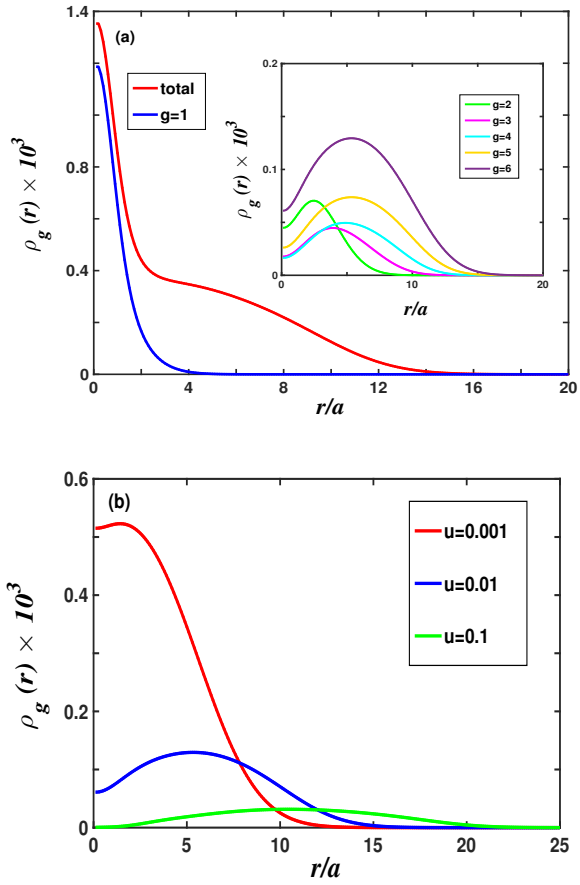

FIG. 4. (a) The segment number density $\rho_g(r)$ with $g = 1 \sim 6$ of the $G = 6$ and $P = 5$ dendron with $u = 0.01$; (b) $\rho_g(r)$ of $g = 6$ of $G = 6$ and $P = 5$ dendron with different u.

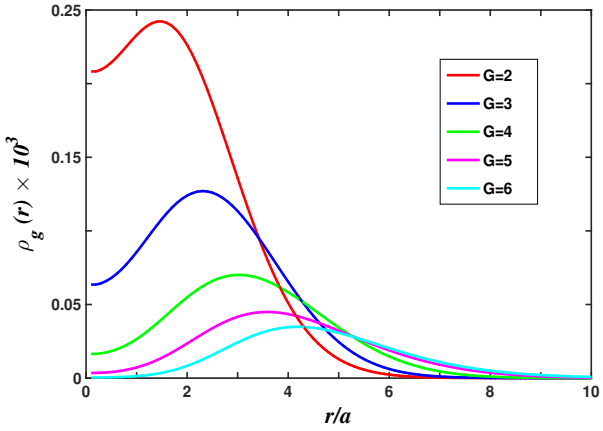

FIG. 5. The segment number density $\rho_g(r)$ of $g = 2$ of $P = 5$ dendrons with $u = 0.1$. The generation number of the dendron varys from $G = 2$ to $G = 6$.

C. The stretched conformation

The equilibrium conformation of a dendron in good solvent is determined by the compromise between entropic energy and volume exclusion energy. The conformation of the flexible spacer stretches to suppress the local segment density, so as to decrease the two-body interaction energy in the cost of increasing entropic energy due to the deviation from an ideal Gaussian chain. The constriction force arising from entropy countervails the stretching force arising from volume exclusion. Certainly, the degree of stretching depends on the topological position as well as the spacial position of a spacer.

In order to analyze the stretching of the spacers, we calculate the distribution of their ends and the the branch points. According to the initial condition of the diffusion equation Eqn. 13, the density function of the first segment $\rho_{p=0}(r)$ is the Dirac delta function at origin $r = 0$. As shown in Fig. 6(a), the density distribution of the branch points $\rho_p(r)$ expends wider with larger p value. This is a straight forward result of increasing side chain length pP. For ideal chain with $u = 0$, the distribution of p-th branch monomer is a Gaussian distribution with the expectation at $r = 0$ and the width $(pP)^{1/2}a$, as shown in Eqn. 19. However, when $u \neq 0$, the peak position obviously increases with p, which indicates the stretched conformation of the spacers. The higher value of the volume exclusion interaction parameter u is, the position of the $\rho_p(r)$ peak moves outwards further, as shown in Fig. 6(b), which verifies the essential influence of volume exclusion on stretching conformation directly. If we increase the generation number of the dendron, which increases the average segment density, the stronger stretching also moves the $\rho_p(r)$ peak further away from the center, as shown in Fig. 6(c).

A nontrivial phenomenon to mention is that the branch point density $\rho_p(r)$ never vanishes at $r = 0$, the center of dendron. This is an important evidence for the back-folding conformation. The back-folding phenomenon was reported in previous experimental[6] and theoretical works[2,18,19,23,34]. We find that even the penetration of good solvents and the excluded volume effect drive the dendron to stretch outwards extensively, the back-folding of the conformation persists. $\rho_p(r)$ decreases with increasing p with the exception of $p = G$, as shown in Fig. 6(a). The terminal $p = G$ segments are free ends which have stronger ability to fold back than the neighbor branch monomer $p = G-1$. Nevertheless, the density of the terminal segment at center decreases with increasing u and G and approaches vanishing (Fig. 6(b,c)). This indicates the possibility to drive the terminal segments away from the center region of dendron with sufficient interaction.

In order to analyze the stretching conformation of the linear side chain directly, we calculate the mean square distance between the first monomer $p = 0$ and the p-th branch point, denoted as R_p. R_p, normalized by the mean end-to-end distance $(pP)^{1/2}$ of a Gaussian dendron, is drawn as a function of p, as shown in Fig. 7(a). Inter-

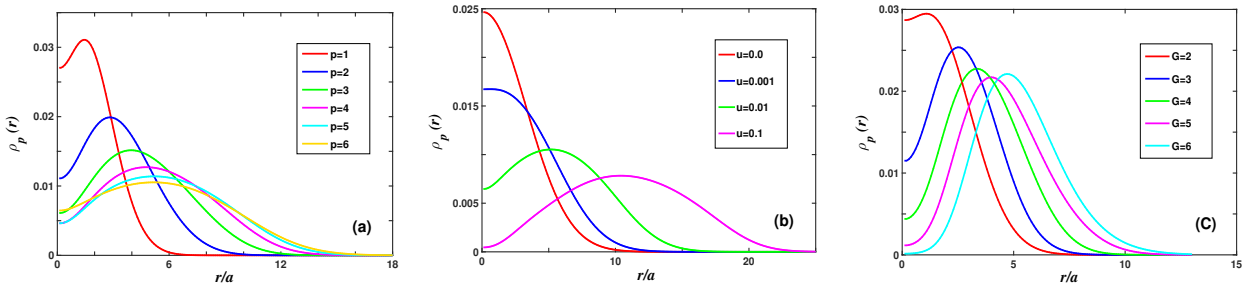

FIG. 6. The density profile of branch monomer $\rho_p(r)$ of a $P = 5$ dendron. (a) $p = 2 \sim 6$ with $G = 6$ and $u = 0.1$; (b) $p = 6$ with $G = 6$ and $u = 0.0, 0.001, 0.01, 0.1$; (c) $p = 2$ with $G = 2 \sim 6$.

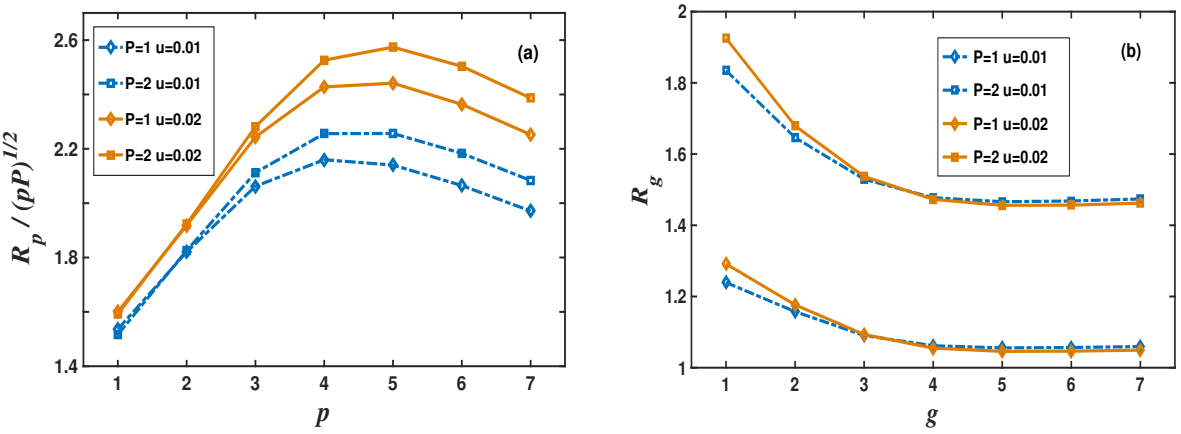

FIG. 7. (a) The mean distance R_p between the first segment and the p-th branch point of a $G = 7$ dendron. (b) The end-to-end distance R_g of the g-th generation spacer of the dendrons as same as in (a).

estingly, $R_p(pP)^{-1/2}$ increases linearly with p near the dendron center, while decreases smoothly after a peak near $p = 4, 5$ when $G = 7$ and $u \sim 10^{-2}$. Such a non-monotonic behavior indicates the non-uniform volume exclusion environment inside the dendron.

We also analyze the end-to-end distance of the g-th generation spacer between the branch points $p = g - 1$ and $p = g$, denoted as R_g. As shown in Fig. 7(b), R_g decreases monotonously as g increases. The spacer of the first generation stretches so strong that R_g is about 30% larger than Gaussian chain of length P, although the value of u is a very finite number of 10^{-2}. After several generations (in Fig. 7(b), about $g = 4$), R_g converges to a constant value slightly larger than $\sqrt{P}$. Combining the information from Figs. 7(a) and (b), we conclude that the stretching behavior is inhomogeneous along the linear side chain. The spacer of the first generation stretches most strongly, because it is localized at the center of the molecule, where the volume exclusion is not only contributed by itself, but also by other spacers penetrating into the center region via the back-folding conformation. The other spacers of small g (e.g. $g = 2$ and $g = 3$ spacers in Fig. 7) are strongly influenced by the densed region near the center. Thus the degree of their stretching depends on the topological distance to the center. The larger g value is, the weaker the spacer stretches. For the spacers of large g (e.g. $g \geq 5$ in Fig. 7), who mainly contributes to the shoulder region of the total monomer density (Fig. 4(a)), the homogeneous extension of the chains implies the irrelavance of topological position to the chain conformation. Therefore, our SCFT calculation with the pre-averaged volume exclusion gives the conformation information of a dendron: near the center region, the chains are elongated, while in the outer region, the spacers behave like flexible chains. This is just the opposite side of the assumption of "hollow-core" model[10].

Note that R_p and R_g are analyzed in radial direction in the sphere coordination. Therefore, we only discuss the radial stretching of the dendron conformation, while the deformation of the conformation in longitude and latitude directions are not of focus here.

D. Scaling law analysis

Via the Flory mean-field theory approach, we obtain the scaling relation $R \sim u^{1/5}(PG)^{1/5}N^{2/5}$, as shown in Eqn. 3. Since N is proportional to P, $R \sim P^{3/5}$ when

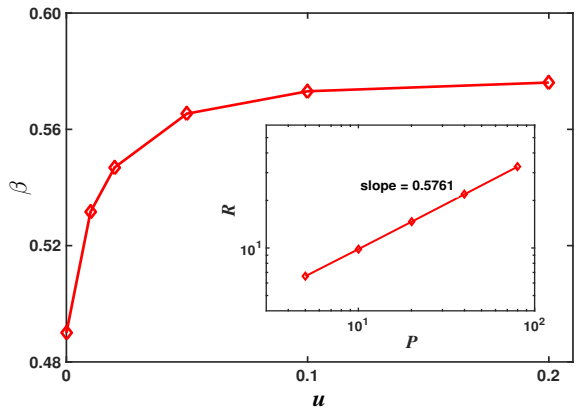

FIG. 8. The scaling exponent β of $R \sim P^{\beta}$ against different u of $G = 4$ dendron. The inset is the R-P plot with $u = 0.2$.

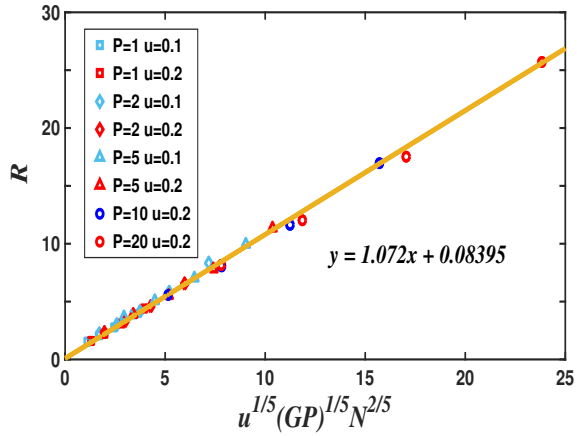

FIG. 9. The scaling relation $R \sim u^{1/5}(GP)^{1/5}N^{2/5}$ of dendrons of $G = 2 - 6$. The insert equation is a linear fit of all data shown here.

G is fixed. This agrees with pioneer researches on the scaling law for good solvent[15,18].

We use the $G = 4$ dendron as an example to show the scaling relation between R and P, as shown in Fig. 8. The solvent parameter starts from the Θ solvent ($u = 0$), and increases to approaching the good solvent limit $u = 0.5$. With each u value, we analyze the scaling behavior $R \sim P^{\beta}$ and plot the exponent β as a function of u. β starts from 0.5 at $u = 0$, which agrees with the ideal Gaussian dendron limit. With increasing u, β increases and converges to a limit value $\beta = 0.58 \pm 0.02$, which is very close to our MF theory prediction $R \sim P^{3/5}$. Moreover, Fig. 8 indicates that only when u is sufficiently large ($u \geq 0.1$), the behavior of the dendron obeys the good solvent scaling laws.

Then, we analyze the scaling relation $R \sim u^{1/5}(GP)^{1/5}N^{2/5}$. We only consider the dendron systems obeying the good solvent scaling laws, i.e. $u = 0.1$ and $u = 0.2$. As shown in Fig. 9, a linear function describes very well the relation between R and $u^{1/5}(GP)^{1/5}N^{2/5}$, no matter how we change G or P and consequently change N. This validates our scaling law obtained via Flory mean-field theory approach. Therefore, suggested by the Flory mean-field theory calculation and supported by our SCFT results, we verify the scaling law relation $R \sim (GP)^{1/5}N^{2/5}$ in the good solvent limit.

IV. SUMMARY AND CONCLUSIONS

In summary, we investigate the conformational behavior and scaling laws of dendrons immersed in a good solvent by using Flory mean-field theory and SCFT method. Our SCFT approach takes into account the excluded volume effect by using a pre-averaged potential describing the two-body interaction between monomers. We confirm the "dense-core" model of dendrons, accompanied by a persistent backfolding conformation, which never disappears with changing volume exclusion effect or solvent property. However, sufficiently strong volume exclusion depresses the density of the terminal monomers near the center, which provides the potential usage in drug delivery system. By analyzing the end-to-end distance of spacers of different generations, we find that different parts of a linear side chain of a dendron are under different stretching conditions. Near the center of the dendron, the spacers are stretched strongly due to the volume exclusion effect of densed, localized monomers at the center. The stretching effect fades quickly with increasing the generation number of the spacer, and approaches to a limit number. Therefore, for the spacers with large generation numbers, which are far from the center and mainly contribute to the shoulder region of the total monomer density, the stretching is relatively weak and homogeneous. Last but not least, our SCFT results support very well our scaling calculation via the Flory mean-field theory approach. At good solvent limit, we find the dendron size R is proportional to $(GP)^{1/5}N^{2/5}$. If we fix G, the scaling law is simplified as $R \sim P^{3/5}$, because N is proportional to P.

Although we have only calculated the conformation of a dendron molecule, which is the primary branch of a dendrimer, our conclusions can be directly applied to dendrimers. A dendron can be considered as a dendrimer of H-shaped core with a small spacer suspended at the center. Comparing with the huge molecule, the suspension chain only enhances the central density peak, and is impossible to strongly influence the other properties such as the scaling behavior and the stretching conformation.

Our future study interest is on the systems of confined dendron with interactions between spacers. The complex morphology is the balance of competition between the entropic depression of spacial confinement, the interfacial energy and the strong volume exclusion effect of the highly fractal configuration.

ACKNOWLEDGMENTS

We are grateful for the financial support from the National Nature Science Foundation of China (Grant No. 21320102005).

[1] G. E. Buhleier, W. Wehner, and F. Vögtle, Synthesis **2**, 155 (1978).
[2] C. Jana, G. Jayamurugan, R. Ganapathy, P. K. Maiti, N. Jayaraman, and A. K. Sood, Journal of Chemical Physics **124**, 204719 (2006).
[3] L. Porcar, K. Hong, P. D. Butler, K. W. Herwig, G. S. Smith, Y. Liu, and W. R. Chen, Journal of Physical Chemistry B **114**, 1751 (2010).
[4] T. J. Prosa, B. J. Bauer, and E. J. Amis, Macromolecules **34**, 4897 (2001).
[5] D. Pötschke, M. Ballauff, P. Lindner, M. Fischer, and F. Vögtle, Journal of Applied Crystallography **33**, 605 (2000).
[6] S. Rosenfeldt, N. Dingenouts, M. Ballauff, N. Werner, F. Vögtle, and P. Lindner, Macromolecules **35**, 8098 (2002).
[7] F. Mallamace, E. Canetta, D. Lombardo, A. Mazzaglia, A. Romeo, L. M. Scolaro, and G. Maino, Physica A **304**, 253 (2002).
[8] T. J. Prosa, B. J. Bauer, E. J. Amis, D. A. Tomalia, and R. Scherrenberg, Journal of Polymer Science: Part B: Polymer Physics **35**, 2913 (1997).
[9] S. Rathgeber, M. Monkenbusch, M. Kreitschmann, V. Urban, and A. Brulet, Journal of Chemical Physics **117**, 4047 (2002).
[10] P. de Gennes and H. Hervet, Journal de Physique Lettres **44**, L351 (1983).
[11] R. L. Lescanec and M. Muthukumar, Macromolecules **23**, 2280 (1990).
[12] M. L. Mansfield, L. I. Klushin, and L. I. Klushint, Macromolecules **26**, 4262 (1993).
[13] M. L. Mansfield and M. Jeong, Macromolecules **35**, 9794 (2002).
[14] Z. Y. Chen and S.-M. Cui, Macromolecules **29**, 7943 (1996).
[15] M. Muratt and G. S. Grest, Macromolecules **29**, 1278 (1996).
[16] D. Boris and M. Rubinstein, Macromolecules **29**, 7251 (1996).
[17] A. V. Lyulin, G. R. Davies, and D. B. Adolf, Macromolecules **33**, 6899 (2000).
[18] Y. J. Sheng, S. Y. Jiang, and H. K. Tsao, Macromolecules **35**, 7865 (2002).
[19] I. O. Götze and C. N. Likos, Macromolecules **36**, 8189 (2003).
[20] E. G. Timoshenko, Y. A. Kuznetsov, and R. Connolly, Journal of Chemical Physics **117**, 9050 (2002).
[21] J. T. Bosko and J. R. Prakash, Macromolecules **44**, 660 (2011).
[22] W. Cui, C. F. Su, H. Merlitz, C. X. Wu, and J. U. Sommer, Macromolecules **47**, 3645 (2014).
[23] J. S. Klos and J. U. Sommer, Macromolecules **46**, 3107 (2013).
[24] T. Lewis, V. Pryamitsyn, and V. Ganesan, Journal of Chemical Physics **135**, 204902 (2011).
[25] Y. Lu, L. An, and Z. G. Wang, Macromolecules **46**, 5731 (2013).
[26] T. Mandal, C. Dasgupta, and P. K. Maiti, Journal of Chemical Physics **141**, 144901 (2014).
[27] A. M. Rubio, C. McBride, and J. J. Freire, Macromolecules **47**, 5379 (2014).
[28] D. Astruc, E. Boisselier, and C. Ornelas, Chemical Reviews **110**, 1857 (2010).
[29] L. Vincent, J. Varet, J.-Y. Pille, H. Bompais, P. Opolon, A. Maksimenko, C. Malvy, M. Mirshahi, H. Lu, J.-P. Vannier, C. Soria, and H. Li, International journal of cancer **105**, 419 (2003).
[30] S. Jain, A. Kaur, R. Puri, P. Utreja, A. Jain, M. Bhide, R. Ratnam, V. Singh, A. S. Patil, N. Jayaraman, G. Kaushik, S. Yadav, and K. L. Khanduja, European Journal of Medicinal Chemistry **45**, 4997 (2010).
[31] U. Boas and P. M. Heegaard, Chemical Society Reviews **33**, 43 (2004).
[32] C. Chen, P. Tang, F. Qiu, and A.-C. Shi, Journal of Chemical Physics **142**, 124904 (2015).
[33] W. R. Chen, L. Porcar, Y. Liu, P. D. Butler, and L. J. Magid, Macromolecules **40**, 5887 (2007).
[34] G. Giupponi and D. M. A. Buzza, Journal of Chemical Physics **120**, 10290 (2004).
[35] P. J. Flory, *Principles of Polymer Chemistry* (Cornell University Press, 1953).
[36] M. L. Mansfield, Polymer **35**, 1827 (1994).
[37] M. W. Matsen, Journal of Physics: Condensed Matter **14**, R21 (2002).
[38] G. Fredrickson, *The Equilibrium Theory of Inhomogeneous Polymers* (Oxford University Press, New York, 2006).
[39] S. F. Edwards, Proceedings of the Physical Society **85**, 613 (1964).
[40] M. Rubinstein, *Polymer Physics* (Oxford University Press, New York, 2003).